Ocean barrier layers' effect on tropical cyclone intensification

Karthik Balaguru[a,b], Ping Chang[b,c,d,1], R. Saravanan[c], L. Ruby Leung[a], Zhao Xu[b,d], Mingkui Li[d], and Jen-Shan Hsieh[c]

[a]Atmospheric Sciences and Global Change Division, Pacific Northwest National Laboratory, Richland, WA 99352; [b]Department of Oceanography, Texas A&M University, College Station, TX 77843; [c]Department of Atmospheric Sciences, Texas A&M University, College Station, TX 77843; and [d]Physical Oceanography Laboratory, Ocean University of China, Qingdao, Shandong 266003, People's Republic of China

Edited by Kerry A. Emanuel, Massachusetts Institute of Technology, Cambridge, MA, and approved July 13, 2012 (received for review January 25, 2012)

Improving a tropical cyclone's forecast and mitigating its destructive potential requires knowledge of various environmental factors that influence the cyclone's path and intensity. Herein, using a combination of observations and model simulations, we systematically demonstrate that tropical cyclone intensification is significantly affected by salinity-induced barrier layers, which are "quasi-permanent" features in the upper tropical oceans. When tropical cyclones pass over regions with barrier layers, the increased stratification and stability within the layer reduce storm-induced vertical mixing and sea surface temperature cooling. This causes an increase in enthalpy flux from the ocean to the atmosphere and, consequently, an intensification of tropical cyclones. On average, the tropical cyclone intensification rate is nearly 50% higher over regions with barrier layers, compared to regions without. Our finding, which underscores the importance of observing not only the upper-ocean thermal structure but also the salinity structure in deep tropical barrier layer regions, may be a key to more skillful predictions of tropical cyclone intensities through improved ocean state estimates and simulations of barrier layer processes. As the hydrological cycle responds to global warming, any associated changes in the barrier layer distribution must be considered in projecting future tropical cyclone activity.

Tropical cyclones (TCs), one of the most devastating and arguably most recurring natural disasters, cause significant damage to life and property annually in many countries worldwide (1, 2). There also is mounting evidence pointing toward potentially important interactions between TCs and climate (3). With the dawn of the satellite era, improved remote-sensing capabilities, in tandem with advanced scientific techniques (4), have contributed to dramatic improvements in predicting the trajectory of a TC. However, to this day, the largest uncertainty resides in the prediction of TC intensity (5). Several previous studies showed that the surface cooling induced by TCs has a significant effect on their intensity (6–8). The intensity of a TC is critically dependent on the air–sea enthalpy difference (9). Thus, any process or feature that can affect the TC-induced sea surface temperature (SST) change due to entrainment caused by wind mixing or upwelling (10) may play a role in TC intensification (11–13), making it critical to understand the factors controlling the upper-ocean response to TCs (14).

The oceanic mixed layer, typically defined as a layer of uniform density and temperature, acts as an interface for air–sea interactions. However, in regions of high fresh water input where the uniform density mixed layer becomes shallower than the uniform temperature isothermal because of salinity influence, the region between the base of the mixed layer and the base of the isothermal layer is defined as the barrier layer (BL) as it acts as a "barrier" to entrainment cooling and vertical mixing (15). Because the BL is a prominent feature of warm regions of the tropical ocean, where TCs are active, they may occur along their tracks. Here, we used a host of in situ and reanalysis datasets combined with output from a high-resolution coupled model to systematically quantify the impact of BLs on TC intensification in major tropical ocean basins. To this end, we performed a Lagrangian computation of SST change, enthalpy flux exchange, and intensification factor under TCs and related them to the presence or absence of BLs (see *Methods*). We begin with an example that served as the motivation for us to conduct this study.

Analysis

Omar was a Category 4 hurricane that occurred in the Caribbean Sea between October 13–18, 2008, reaching a maximum sustained wind speed of about 215 $km\,hr^{-1}$. Fig. 1*A* shows the SST change caused by Omar, while Fig. 1*B* shows the pre-existing barrier layer thickness (BLT) (*Methods*). Initially, as Omar began to develop, it caused considerable SST cooling of nearly 1.5 °C in a region without significant BLs. Then, it gradually entered a region with deep BLs, up to 30 m in maximum thickness, where the SST cooling was substantially reduced or SST change was even weakly positive. Finally, as it exited this region and entered a region without prominent BLs, intense surface cooling resumed. These observations point to the possibility that the presence of thick BLs may have been responsible for the reduction in SST cooling caused by Omar.

A pair of Argo floats (16) happened to be located very close to Omar's track. The first one was located at 67.4 °W, 14.9 °N, approximately 12 km away from Omar's path. The float profiled the ocean at about the same time (10/15/2008, 12 PM) Omar passed near it. Thus, it provided real-time information about the prevailing oceanic conditions during Omar's passage. Fig. 1*C* shows the sub-surface salinity and temperature recorded by the float with the density, mixed layer depth (MLD), and isothermal layer depth (ILD) indicated (also see Fig. S1). The MLD was about 51 m deep, and below it there was a BL nearly 15 m in thickness. Within the BL, the temperature inversion was nearly 0.3 °C in magnitude. The second float, located at 61.9 °W, 19.5 °N and about 22 km from the hurricane's track, was able to measure the ocean state on October 16, 2008, at about the same time (10/16/2008, 12 PM) the hurricane passed by it. Fig. 1*D* shows the hydrographic conditions measured by the float. It shows that there was a large sub-surface salinity maximum at a depth of about 10 m. Due to this salinity effect, the MLD was shallower than 10 m, resulting in a thick BL with a depth exceeding 30 m. However, the BL found in this case is not a typical BL (additional discussion in *SI Text*). Within the BL, there was a substantial temperature inversion of almost 1 °C. Thus, it is conceivable that when a TC passes over such oceanic regions, the mixing induced by it can cause the warmer pycnocline water to enter the mixed layer,

---

Author contributions: K.B. formulated the initial idea, methodology, and performed the observational analysis; P.C. directed the research and refined the ideas, methods, and interpretation of results; K.B., P.C., R.S., and L.R.L. wrote the paper; Z.X. performed the analysis of model data; and M.L. and J.-S.H. conducted the model simulations.

The authors declare no conflict of interest.

This article is a PNAS Direct Submission.

Freely available online through the PNAS open access option.

[1]To whom correspondence should be addressed. E-mail: ping@tamu.edu.

This article contains supporting information online at www.pnas.org/lookup/suppl/doi:10.1073/pnas.1201364109/-/DCSupplemental.

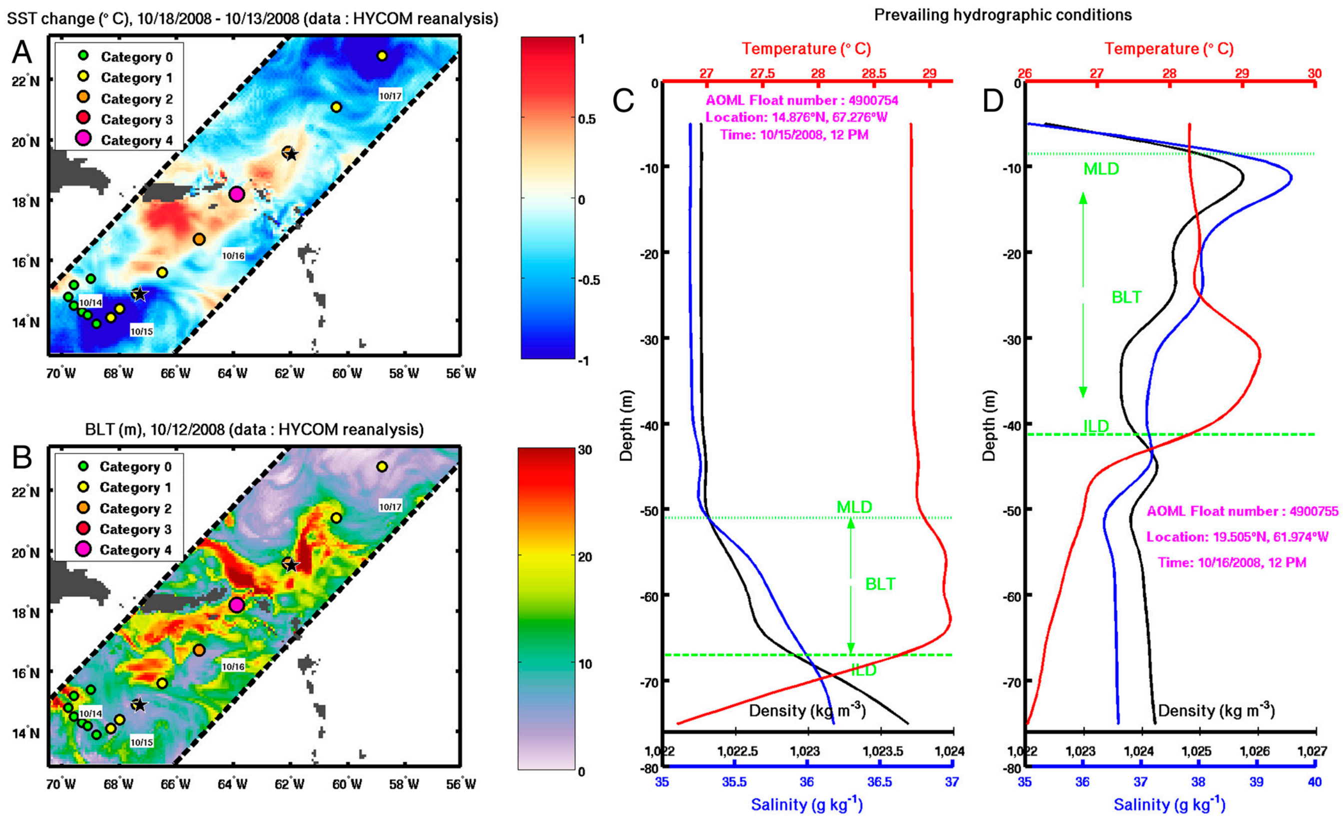

Fig. 1. The path of Hurricane Omar (colored dots) overlaid on (*A*) the difference of SST between October 13–18, 2008, and (*B*) the pre-existing BLT (October 12, 2008). The legend in each figure corresponds to categorization of the strength of Omar based on the Saffir–Simpson scale, while the color bar indicates the magnitudes of SST change (°C) and BLT (m) in the respective figures. The black star indicates the location of Argo floats. The black dotted lines enclose the region influenced by the hurricane, which is approximately 400 km wide. The sub-surface temperature, salinity, and density profiles measured by Argo floats (*C*) 4900754 on October 15, 2008, at 67.4 °W and 14.9 °N and (*D*) 4900755 on October 16, 2008, at 61.9 °W and 19.5 °N. The dotted line and dashed lines indicate the MLD and ILD, respectively, with the distance separating them being the BLT.

resulting in a reduced SST cooling or even a slight warming, as shown in Fig. 1*A*. A similar effect has been noted in the extratropics, where mixing due to polar lows can lead to surface warming and consequently their intensification (17). In the tropics, although the maximum magnitude of temperature inversions is about 0.5–1 °C, they may have a similar effect on enthalpy flux transfer during a TC event.

Does the effect of BLs on TC-induced SST change hold true in general, and does this effect have an impact on TC intensification? To address this, we analyzed a decade of TC tracks from 1998 to 2007 in the major tropical BL regions, which included a total of 587 TCs (Table 1) in the northwestern and southwestern tropical Pacific, northwestern tropical Atlantic, and northern tropical Indian Ocean basins. Fig. 2*A* illustrates all of the TC tracks used in our analysis with the TC season-averaged BLT shown in the background. To evaluate the effect of BLs on TCs, we computed the SST change, enthalpy flux transfer at the air–sea interface, and intensification factor for each slow-moving point along the tracks of these TCs. As it is well known that air–sea coupling effects begin to assume significance for the surface ocean response to TCs and for TC intensification only when the storm moves slowly (8, 10), we considered only those locations where the TC translational speed is small (*Methods*). We further subsampled the data for analysis using a minimum SST criterion to isolate the BL effect from other factors that can affect TC intensification (*Methods*). Tropical BLs predominantly occur in regions where the ocean is warmer, and TC characteristics may be significantly different from those in non-BL regions. Choosing an SST criterion that requires prestorm SST for the BL and non-BL sample sets above a certain value confines the selected TCs to within approximately the same geographic regions and thus allows us to avoid these sampling issues. When the minimum SST criterion was satisfied, we found the difference in TC maximum wind speed and translation speed became statistically insignificant between the BL and non-BL sample sets, so the influence of other factors on TC intensification is minimized. Lagrangian composites were

Table 1. BL effect on TC intensification in different tropical ocean basins*

	Ocean Basin	No. of TCs	Mean TC intensification factor over BL regions (m s^{-1} per 36 h)	Mean TC intensification factor over non-BL regions (m s^{-1} per 36 h)	Probability of TC-BL interaction
1	Northwestern Tropical Pacific	292	1.29	1.10	0.14
2	Northwestern Tropical Atlantic	150	0.98	0.48	0.10
3	Southwestern Tropical Pacific	93	2.53	1.36	0.23
4	Northern Tropical Indian	52	1.29	0.59	0.10

*The number of TCs analyzed, mean TC intensification factor over BL and non-BL regions and the probability of TC-BL interaction, which is the ratio between the number of BL points and the total number of points, for the decade 1998–2007 in each ocean basin

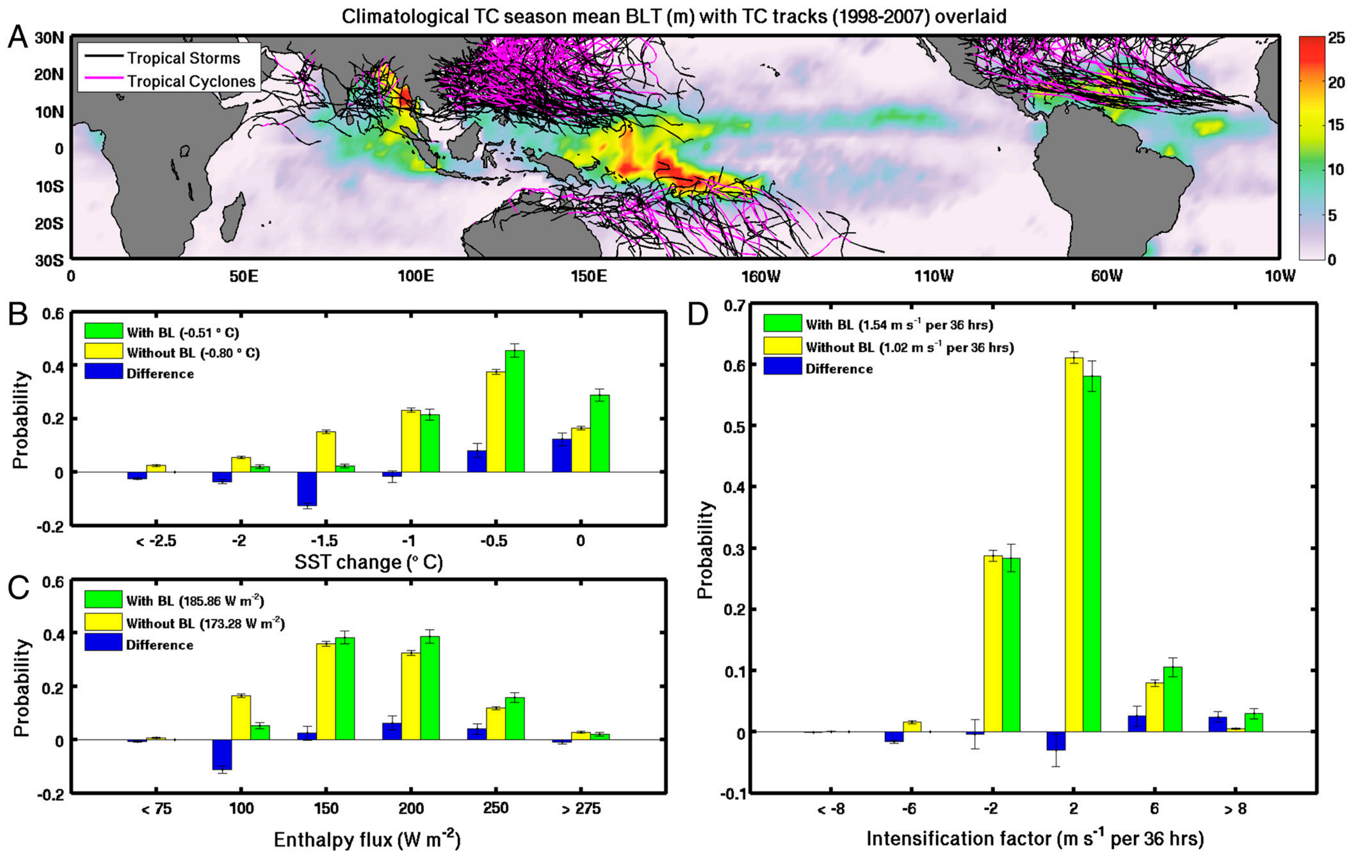

Fig. 2. (*A*) An illustration of the TC tracks used in this analysis with the TC season (May–December for the Northern and October–April for the Southern hemispheres, respectively) averaged BLT (m) in the background. The color bar corresponds to the magnitude of BLT (m), while the legend corresponds to the strength of TCs. Probability distribution functions, or PDFs, of (*B*) SST change induced by TCs, (*C*) enthalpy flux exchange at the air–sea interface under TCs, and (*D*) TC intensification factor with error bars indicated. The mean values of SST change, enthalpy flux exchange, and intensification factor in the presence and absence of BLs are shown in the legends of the respective figures.

made by sub-dividing TCs into two groups—those passing over a BL and those not passing over a BL. Fig. 2 shows the probability distribution functions (PDFs) generated from the composite analysis. It is evident that the BL PDFs are skewed to the right compared to the non-BL PDFs, suggesting that in the presence of BLs, the enhanced salinity stratification within the isothermal layer lowers the vertical mixing caused by TCs. This results in reduced SST cooling and an increased enthalpy flux transfer into the atmosphere leading to TC intensification. Due to the BL effect, the mean SST cooling induced by TCs is reduced by 36%, and the mean flux of enthalpy heat drawn out of the ocean by TCs increases by 7%. The mean intensification factor for TCs over non-BL regions is 1.02 $\mathrm{m\,s^{-1}}$ per 36 hrs, while it is 1.54 $\mathrm{m\,s^{-1}}$ per 36 hrs for TCs over BLs—nearly 1.5 times higher—making the BL effects on TC intensification prominent even though the probability of TC-BL interaction ranges between 10–23% in each basin.

Model

A comparative analysis conducted for TCs with and without the BL effect using simulations from a high-resolution regional coupled model further substantiated our results. A total of 315 simulated TCs were analyzed (*SI Text*). Fig. 3*A* shows the simulated mean BLT overlaid by the tracks of strong simulated hurricanes (Category 2). Despite the underestimated TC intensity, the model captures the observed BL structure and TC tracks reasonably well. It also shows that BL-associated temperature inversions contribute to SST warming during TC events (Fig. S2). Fig. 3*B* shows the composite sub-surface temperature response to TC-induced mixing. There is considerable surface cooling with a maximum of nearly 1 °C, situated at about 50 km to the right of the storm center, consistent with the well-known rightward shift in maximum cooling in the northern hemisphere (10). The effect of BLs on the upper-ocean temperature response is shown in Fig. 3*C*, which illustrates the difference between the BL and non-BL composites. Clearly, in the presence of BLs, there is a relative warming in the surface layer of the ocean compared to the case without BLs, and the maximum cooling to the right is reduced by nearly 40%. Consistent with the reduced cooling, composite profiles of simulated vertical turbulent heat flux show that the mean heat flux, averaged over 50–100 m depth, with BLs (approximately 1,320 $\mathrm{W\,m^{-2}}$) is reduced by nearly 40% compared to the value without BLs (approximately 2,176 $\mathrm{W\,m^{-2}}$) (Fig. 3*D*). PDFs of SST change, enthalpy flux exchange, and TC intensification factor follow a similar pattern as in the observational analyses (Fig. S3). In the presence of BLs, the mean SST cooling reduces by 33%, the mean enthalpy flux transfer increases by 5.3%, and the mean TC intensification factor increases by a factor of 1.7, lending further support to the observational results.

Conclusions and Discussion

While information of upper-ocean thermal structure has been shown to augment the intensity forecast (18), the idea that upper-ocean salinity can also play a role has been hitherto untested at a global scale. Past studies have suggested a potential role of BLs in TC-induced SST cooling (19) and TC intensification (20–22). However, the impact of BLs on TC intensification has not been definitively demonstrated or quantified. Using a string of observations and high-resolution coupled model simulations, we systematically demonstrated that salt-stratified BLs in the tropical

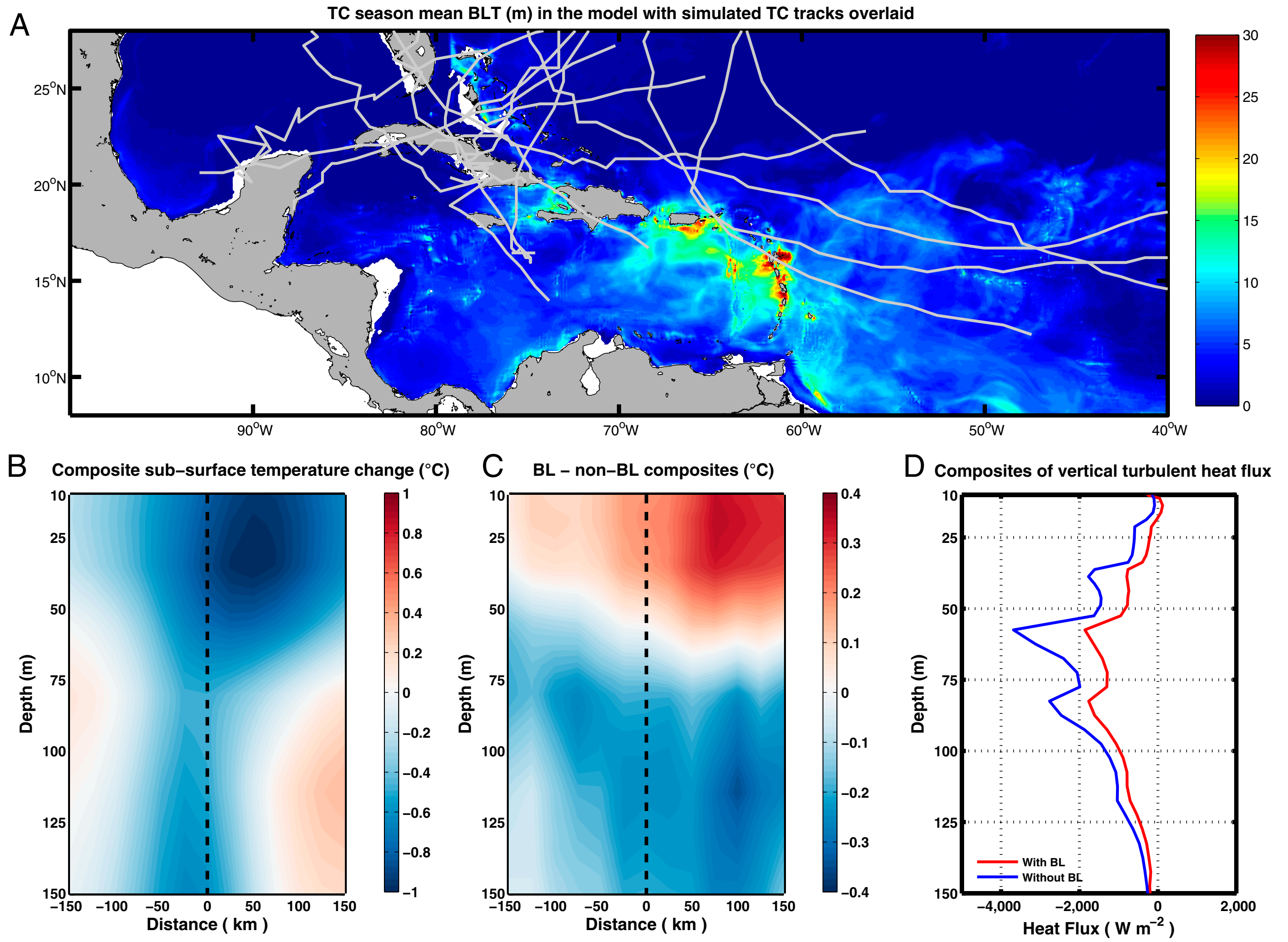

Fig. 3. (*A*) An illustration of BL and TC simulation in the model. The BL shown here is averaged over the months May–September overlaid with tracks of TCs reaching the strength of Category 2. The color bar indicates the magnitude of BLT (m). Sections of composite sub-surface temperature response to TCs from the model (*B*) mean response and (*C*) difference between the BL and non-BL composites. The sections are perpendicular to the direction of the TC (into the page) and centered at its eye. (*D*) Composite mean profiles of TC-induced upward turbulent heat flux for cases with and without BLs at the center of the TC. The profiles are averaged approximately over a radius of 9 km, which is the model horizontal resolution. Only events where the storm reached TC status and was slow moving were used to build these composites.

upper oceans significantly influence TC intensification. When TCs pass over BLs, the reduced efficacy of vertical mixing in their presence leads to reduced SST cooling, which then impacts TC evolution through changes in air–sea enthalpy flux transfer.

Both theory (23) and observations (24) show that a significant majority of the total damages inflicted by TCs is caused by the most intense storms. In light of this and our study, the role of BLs in TC intensification should not be overlooked, as even modest improvements in TC intensity forecast skill can aid societal response and help mitigate these storms' destructive power. Because an understanding of interannual-to-decadal variability in BL conditions also may provide constraints for predicting TC intensities at longer time scales, future model improvements need to consider BL processes in the upper ocean. As the ocean water cycle is projected to change under global warming (25), tropical ocean BLs may also change accordingly. The impact of this BL change on future TCs is an issue that deserves consideration in studies of TC-climate interactions.

Methods

Data. TC track data, obtained from http://eaps4.mit.edu/faculty/Emanuel/products for the period 1998–2007, are used to find TC locations and compute its translation speed (V) and intensification factor. The data herein were compiled from the National Hurricane Center (NHC) and the U.S. Navy's Joint Typhoon Warning Center (JTWC). The wind speeds given in this data are 1-min averaged sustained winds at an altitude of 10 m. To account for errors in methods of wind speed estimation, several wind-speed-dependent corrections have been introduced in this data (23).

Daily SST data, obtained from http://www.esrl.noaa.gov/psd/data (26), are used to compute SST change along TC tracks. Objectively analyzed air–sea fluxes (OAFlux) data, obtained daily from http://oaflux.whoi.edu (27), are used to compute the enthalpy fluxes at the air–sea interface for TCs. A discussion about the limitation of this data product is provided in *SI Text*. The Simple Ocean Data Assimilation, or SODA, an ocean reanalysis pentad data product obtained from http://soda.tamu.edu/ (28), is used to compute pre-existing BLT along TC tracks. Daily ocean reanalysis data, obtained from http://hycom.org/ (29), are used to compute SST changes and pre-existing BLT for the Hurricane Omar case study. In addition, data from several Argo floats (AOML float numbers 4900754, 4900755, 4900800, and 4900572), obtained from http://www.usgodae.org/argo/, are used to examine the sub-surface hydrographic conditions near Omar's path. BLT climatology data, obtained from http://www.lodyc.jussieu.fr/~cdblod/blt.html (30), are used to depict the hurricane season averaged BLT in Fig. 2*A*.

Model. The model simulations analyzed in this study are from an ensemble of 17 runs using a high-resolution coupled regional climate model developed at Texas A&M University (TAMU) (31). Each integration starts from May 1 through end of September and is initiated with perturbed atmospheric initial conditions but identical ocean initial and climatological boundary conditions (refer to *SI Text* for more details).

Calculations. BLT is defined as ILD minus MLD (30) and can exist if it is at least 10 m in magnitude. Model-simulated TC locations are tracked using a well-established TC tracking algorithm (32). Slow-moving TCs are separated from fast-moving ones using the '$\frac{V}{fL} < 1$' criterion, where V is the TC translational speed, f the Coriolis parameter, and L a TC length scale chosen as 100 km (8). SST change at each location along TC tracks is evaluated as the difference between SST two days after the passage of the TC and the average SST over the 10-day period prior to a day before the approaching storm (8). Enthalpy flux along TC tracks is evaluated as the sum of latent and sensible heat fluxes one day after the arrival of the TC. To account for asymmetry in TCs, we used an average over a $4° \times 4°$ box centered at the eye of the storm to compute BLT, SST change, and enthalpy fluxes.

The intensification factor is computed as the linear regression coefficient of the maximum wind speed ($V_{\max}$) over six data points, which includes the current and five subsequent six-hourly snapshots (8). Positive regression coefficient signifies TC intensification, while negative indicates TC decay. The vertical turbulent heat flux is computed as $\rho C_p \kappa_t \frac{dT}{dz}$, where $\rho(\mathrm{kg\,m^{-3}})$ is the seawater density, C_p is the specific heat capacity of seawater ($4{,}000\ \mathrm{J\,kg^{-1}\,K^{-1}}$), κ_t ($\mathrm{m^2\,s^{-1}}$) is the vertical thermal eddy diffusivity, and $\frac{dT}{dz}$ is the vertical temperature gradient at a depth z. The mixed layer-averaged horizontal advective heat flux is calculated as $\rho C_p h \nabla \cdot (\nu_h T_h)$, where ∇ is the horizontal gradient operator, h is the mixed layer depth, and ν_h and T_h are the mixed layer-averaged horizontal velocity vector and temperature, respectively.

To isolate the effects of BLs, we sub-sampled the data using a minimum SST criterion. A lower bound for prestorm SST is employed to consider TC locations so the selected points are confined to nearly the same geographic regions, thus eliminating the influence of other TC characteristics. In our data, we found that using the criterion of SST $\geq$ 28.5 °C, the difference in TC maximum wind speed ($V_{\max}$) and translation speed ($\frac{V}{fL}$) between the BL and non-BL sample sets becomes statistically insignificant at the 95% level based on a Student's t-test. For this reason, the effect of BLs can be explicitly delineated.

The PDFs were computed using a Monte Carlo method. We randomly chose half the elements of the sample set to generate a PDF and repeated this process numerous times (here 100,000). For each bin, the mean and standard deviation of the bin sizes, calculated across the various PDFs, yield the corresponding mean bin size and error. Values reported throughout this paper from various comparative analyses satisfy the one-tailed Student's t-test for difference of means at 95% confidence level ("t" value of 1.65). Hence, they are statistically significant.

ACKNOWLEDGMENTS. This research was funded by U.S. National Science Foundation Grant AGS-1067937, and by the U.S. Department of Energy (DOE) Regional Integrated Assessment Modeling (RIAM) project and DOE Grants DE-SC0004966 and DE-SC0006824. P.C. acknowledges support from the National Science Foundation of China (41028005, 40921004, and 40930844) and the Chinese Ministry of Education's 111 project (B07036). M.L. acknowledges support from the Chinese National Basic Research Program (2012CB417400) and the National Science Foundation of China (41130859). Pacific Northwest National Laboratory is operated by Battelle for the DOE under contract DE-AC05-76RL01830.

1. Emanuel KA (2003) Tropical cyclones. *Annu Rev Earth Planet Sci* 31:75–104.
2. Pielke RA, Jr, Rubiera J, Landsea C, Fernandez ML, Klein R (2003) Hurricane vulnerability in Latin America and the Caribbean: Normalized damage and loss potentials. *Nat Hazards Rev* 4:101–114.
3. Sriver RL, Huber M (2007) Observational evidence for an ocean heat pump induced by tropical cyclones. *Nature* 447:577–580.
4. DeMaria M, Mainelli M, Shay LK, Knaff JA, Kaplan J (2005) Further improvements to the Statistical Hurricane Intensity Prediction Scheme (SHIPS). *Wea Forecasting* 20:531–543.
5. Emanuel KA, DesAutels C, Holloway C, Korty RL (2004) Environmental control of tropical cyclone intensity. *J Atmos Sci* 61:843–858.
6. Bender MA, Ginis I (2000) Real-case simulations of hurricane-ocean interaction using a high-resolution coupled model: Effects on hurricane intensity. *Mon Wea Rev* 128:917–946.
7. Cione JJ, Uhlhorn WE (2003) Sea surface temperature variability in hurricanes: Implications with respect to intensity change. *Mon Wea Rev* 131:1783–1796.
8. Lloyd ID, Vecchi GA (2011) Observational evidence for oceanic controls on hurricane intensity. *J Clim* 24:1138–1153.
9. Emanuel KA (1999) Thermodynamic control of hurricane intensity. *Nature* 401:665–669.
10. Price JF (1981) Upper ocean response to a hurricane. *J Phys Oceanogr* 11:153–175.
11. Shay LK, Goni GJ, Black PG (2000) Effects of a warm oceanic feature on hurricane opal. *Mon Wea Rev* 128:1366–1383.
12. Shen W, Ginis I (2003) Effects of surface heat flux-induced sea surface temperature changes on tropical cyclone intensity. *Geophys Res Lett* 30:1933–1936.
13. Lin I-I, et al. (2005) The interaction of supertyphoon maemi (2003) with a warm ocean eddy. *Mon Wea Rev* 133:2635–2649.
14. Vincent EM, et al. (2012) Assessing the oceanic control on the amplitude of sea surface cooling induced by tropical cyclones. *J Geophys Res* 117:C05023–C05037.
15. Sprintall J, Tomczak MJ (1992) Evidence of the barrier layer in the surface layer of the tropics. *J Geophys Res* 97:7305–7316.
16. Roemmich DH, et al. (2009) The Argo Program: Observing the global ocean with profiling floats. *Oceanography* 22:34–43.
17. Saetra O, Linders T, Debernard JB (2008) Can polar lows lead to a warming of the ocean surface? *Tellus A* 60:141–153.
18. Goni GJ, Trinanes JA (2003) Ocean thermal structure monitoring could aid in the intensity forecast of tropical cyclones. *Eos Trans AGU* 84:573–578.
19. Sengupta D, Goddalehundi BR, Anitha DS (2008) Cyclone-induced mixing does not cool SST in the post-monsoon north Bay of Bengal. *Atmos Sci Letts* 9:1–6.
20. Wang X, Han G, Qi Y, Li W (2011) Impact of barrier layer on typhoon-induced sea surface cooling. *Dyn Atmos Oceans* 52:367–385.
21. Ffield A (2007) Amazon and Orinoco River plumes and NBC Rings: Bystanders or participants in hurricane events? *J Clim* 20:316–333.
22. McPhaden MJ, et al. (2009) Ocean-atmosphere interactions during cyclone nargis. *Eos Trans AGU* 90:53–60.
23. Emanuel KA (2005) Increasing destructiveness of tropical cyclones over the past 30 years. *Nature* 436:686–688.
24. Pielke RA, Jr, et al. (2008) Normalized hurricane damage in the United States: 1900–2005. *Nat Hazards Rev* 9:29–42.
25. Held IM, Soden BJ (2006) Robust responses of the hydrological cycle to global warming. *J Clim* 19:5686–5699.
26. Reynolds RW, et al. (2007) Daily high-resolution blended analyses for sea surface temperature. *J Clim* 20:5473–5496.
27. Yu L, Weller RA (2007) Objectively analyzed air-sea heat fluxes for the global ice-free oceans (1981–2005). *Bull Am Meteorol Soc* 88:527–539.
28. Carton JA, Giese BS (2008) A reanalysis of ocean climate using simple ocean data assimilation (SODA). *Mon Wea Rev* 136:2999–3017.
29. Chassignet EP, et al. (2007) The HYCOM (HYbrid Coordinate Ocean Model) data assimilative system. *J Mar Syst* 65:60–83.
30. de Boyer Montégut C, Mignot J, Lazar A, Cravatte S (2007) Control of salinity on the mixed layer depth in the world ocean. Part I: General description. *J Geophys Res* 112: C06011–C06023.
31. Patricola CM, et al. (2012) An investigation of tropical atlantic bias in a high-resolution coupled regional climate model. *Clim Dyn*, 10.1007/s00382-012-1320-5.
32. Camargo SJ, Zebiak SE (2002) Improving the detection and tracking of tropical cyclones in atmospheric general circulation models. *Wea Forecasting* 17:1152–1162.